

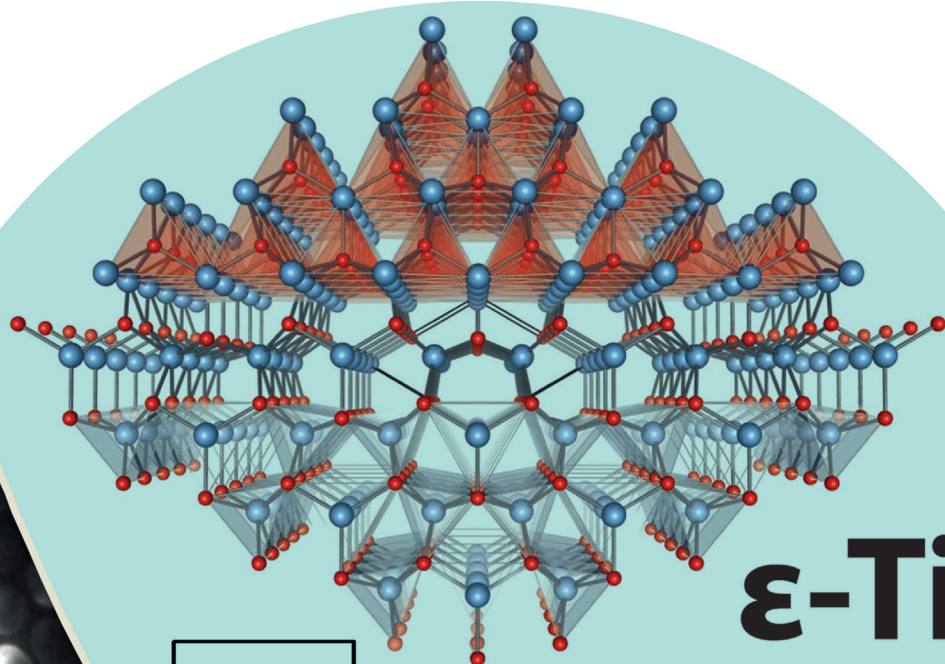
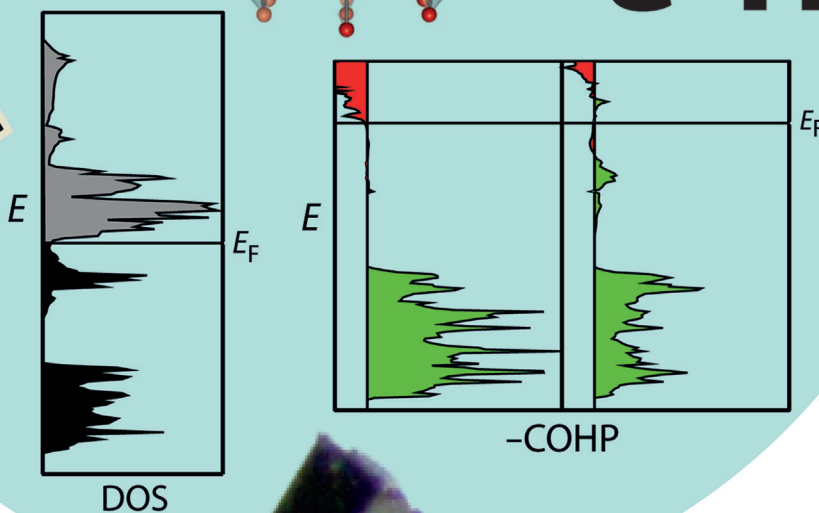


Polymorphism Hot Paper

Deutsche Ausgabe: DOI: 10.1002/ange.201510479
Internationale Ausgabe: DOI: 10.1002/anie.201510479

ϵ -TiO, a Novel Stable Polymorph of Titanium Monoxide

Shinsaku Amano, Dimitri Bogdanovski, Hisanori Yamane,* Masami Terauchi, and Richard Dronskowski*

 ϵ -TiO

Abstract: For the Ti/O system, three titanium monoxide (TiO) phases (α , β , and γ) with defective NaCl-type structures and a high-temperature hexagonal phase (H) have been known for decades. In this work, single crystals of a novel polymorph, ϵ -TiO, were synthesized by using a bismuth flux. X-ray diffraction (XRD) revealed a hexagonal crystal structure ($a = 4.9936(3)$ Å, $c = 2.8773(2)$ Å, $P\bar{6}2m$) that is isotypic with ϵ -TaN. While the Ti atoms are surrounded by trigonal prismatic (sixfold coordination) and trigonal planar (threefold coordination) arrangements of O atoms, the O atoms are found in a pseudo-square-pyramidal arrangement of Ti atoms. First-principles calculations of the formation enthalpy and the electron and phonon density of states and crystal orbital Hamilton population (COHP) analysis revealed that ϵ -TiO is more stable than α -TiO, which had previously been regarded as the most stable phase at low temperatures.

The Ti/O binary system is a representative binary oxide system whose members and phase relations have been investigated for several decades. Aside from the well-known photocatalyst titanium dioxide, TiO₂, various oxides with nonstoichiometry and lower Ti oxidation states, such as Ti₂O, TiO, Ti₃O₅, and Ti₂O₃, and Magnéli phases, Ti_nO_{2n-1} ($4 \leq n \leq 9$), have been reported.^[1–8] In fact, Murray and Wriedt have assessed 138 research papers on the crystal structures and phase relations in the Ti/O system that were published between 1937 and 1984, and they also reported a phase diagram for this system,^[9] which was subsequently re-evaluated by Okamoto in 2011.^[10] We will argue that this very phase diagram is incomplete because the ground-state TiO phase was still missing.

According to the phase diagram, there are three TiO phases, α , β , and γ . In these phases, about 15 at % of both the Ti and O sites are unoccupied, and the stability–defect relationships have been theoretically studied.^[11–15] Whereas γ -TiO is the high-temperature phase with a NaCl-type (rock-salt-type, B1) cubic structure ($Fm\bar{3}m$, $a = 4.184$ Å),^[16,17] cubic β -TiO crystallizes in a superstructure of γ -TiO ($a = 12.54$ Å);^[17] both γ - and β -TiO display wide ranges of nonstoichiometry. The β – γ phase-transition temperature is approximately 1523 K.^[9] α -TiO, however, is the monoclinic low-temperature phase and has an ordered array of vacant lattice sites ($B2/m$, $a = 9.340(5)$ Å, $b = 5.860(4)$ Å, $c = 4.141(1)$ Å, $\gamma = 107.553(6)^\circ$).^[18–20] Here, the Ti and O vacancies alternate in every third (110) plane of the NaCl-type structure. Another hexagonal type of TiO, H-TiO, ($P\bar{6}m2$, $a =$

$3.0310(6)$ Å, $c = 3.2377(9)$ Å) has been synthesized above 3273 K,^[21] and it is isostructural with WC because the Ti atoms are located in sixfold coordination sites of oxygen trigonal prisms. Herein, a new polymorph of titanium monoxide, ϵ -TiO, has been prepared by using a Bi flux. Its crystal structure was determined by single-crystal X-ray diffraction (XRD), and the phase stability and chemical bonding of ϵ -TiO were investigated by electronic-structure calculations.

Samples containing single crystals of ϵ -TiO were prepared by heating Bi, Bi₂O₃, and Ti with a Ti/O molar ratio of 1.0:0.9 at 1173 K for two hours, followed by slow cooling to 773 K. The samples obtained after Bi removal by washing with an aqueous solution of nitric acid and water were mixtures of metallic silver-black prismatic or needle-like single crystals with lengths of about 200–900 μ m and dark-brown grains. The latter consisted of 1–2 μ m large microcrystalline particles of previously known TiO phases (mainly γ -TiO as determined by powder XRD, see the Supporting Information, Table S1 and Figures S1, S2 a).

Only Ti and O were detected in the prismatic single crystals and grains by means of wavelength-dispersive X-ray (WDX) spectroscopy. The composition of the prismatic single crystals analyzed by WDX was 75.0(4) wt % Ti and 26-(2) wt % O (overall 101(2) %). The Ti/O molar ratio of the single crystals was 1:1 within experimental error. The Ti/O molar ratio of the grains on the single crystals was also close to 1:1.

The main peaks in the powder XRD pattern of the sample could be indexed to hexagonal cell parameters as determined by single-crystal XRD ($a = 4.9936(3)$ Å, $c = 2.8773(2)$ Å; Figure S2 a). The cell parameters were close to those of TiO_{0.5} (hexagonal $P6/mmm$, $a = 4.991(5)$ Å, $c = 2.879(4)$ Å) reported by Andersson.^[22] Nonetheless, the compositions of the two compounds were different. Thus the new hexagonal phase was termed ϵ -TiO. The XRD peaks of the α - and γ -TiO side phases were also seen in the XRD pattern.

Single crystals of ϵ -TiO were also prepared by using TiO₂ instead of Bi₂O₃ as an oxygen source with a starting molar ratio of Ti/O = 1.0:1.0. When the sample was prepared with a powdery pellet of Ti and TiO₂ (Ti/O = 1.0:1.0) without Bi, the product consisted of Ti₂O, γ -TiO, and Ti₂O₃, but not ϵ -TiO. On the other hand, fine single crystals of ϵ -TiO with a size below 30 μ m were obtained as the main phase by heating a powdery mixture of Ti and Bi₂O₃ (Ti/O = 1.0:1.0) and washing it with HNO₃ and water. The Bi melt was formed by reduction of Bi₂O₃ with Ti metal. These results indicate that a Bi flux (m.p. 544.8 K) is necessary to crystallize ϵ -TiO, and it becomes clear why the phase has been overlooked thus far.

The crystal structure of ϵ -TiO was determined by XRD using the APEX2^[23], SHELXL-97,^[24] and VESTA^[25] packages, as further detailed in the Supporting Information. The structure model of ϵ -TaN (space group $P\bar{6}2m$)^[26] was adopted, yielding an R 1 value (2σ) of 1.13 % and an S value of 1.144 (Tables S2–S4).^[27] As no other binary compound with the structure type of ϵ -TaN was found in the Inorganic Crystal Structure Database (ICSD), ϵ -TiO is probably only the second example.

[*] S. Amano, Prof. Dr. H. Yamane, Prof. Dr. M. Terauchi
Institute of Multidisciplinary Research for Advanced Materials
Tohoku University
2-1-1 Katahira, Aoba-ku, Sendai 980-8577 (Japan)
E-mail: yamane@tagen.tohoku.ac.jp
D. Bogdanovski, Prof. Dr. R. Dronskowski
Institute of Inorganic Chemistry
RWTH Aachen University
Landoltweg 1, 52056 Aachen (Germany)
E-mail: drons@HAL9000.ac.rwth-aachen.de

Supporting information for this article is available on the WWW under <http://dx.doi.org/10.1002/anie.201510479>.

The Ti1 site of ϵ -TiO is surrounded by six O atoms with a triangular-prismatic arrangement and $\text{Ti1-O} = 2.1025(2) \text{ \AA}$ ($\times 6$; Figure 1a, Table S5). In the structure of H-TiO ($P\bar{6}m2$), the Ti atoms are coordinated to the O atoms with the same arrangement, but the Ti–O bonds are longer ($2.3839(4) \text{ \AA}$).^[21] The Ti2 atoms in ϵ -TiO were found to be in a regular triangular O plane with an O–Ti2–O angle of 120° . The Ti2–O bond of $1.9745(8) \text{ \AA}$ coincides with the shortest Ti–O bond of 1.975 \AA in α -TiO.^[20] To the best of our knowledge, a planar triangular threefold coordination of O atoms has not been described for other binary and multinary titanium oxides thus far.

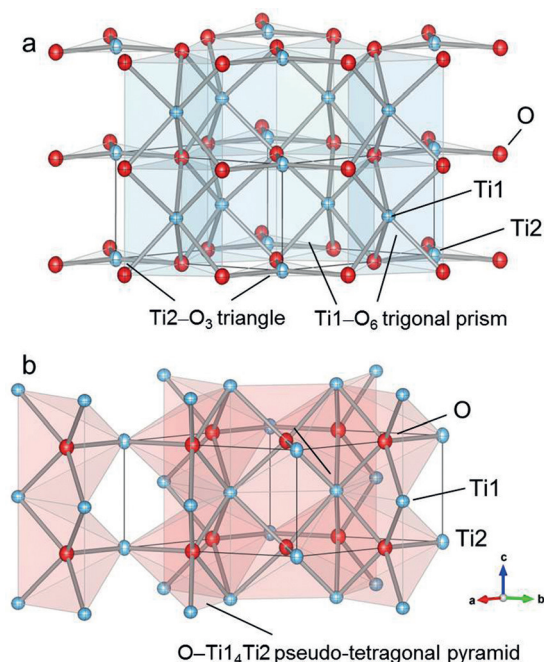


Figure 1. Crystal structure of ϵ -TiO. a) Ti1–O and Ti2–O bonds, Ti1-centered O_6 trigonal prisms, and Ti2-centered O_3 triangles. b) O-centered $(\text{Ti1})_4\text{Ti2}$ pseudo-tetragonal pyramids. Ellipsoids set at 99% probability.

The O atom rests in a square-pyramidal (or pseudo-tetragonal) arrangement of four Ti1 atoms (rectangular base) and one Ti2 atom (Figure 1b). The Ti1–Ti1 distances parallel and perpendicular to the c axis are $2.8773(2) \text{ \AA}$ ($=c$) and $2.8831(2) \text{ \AA}$, respectively, and the base rectangle is almost a square. These Ti–Ti distances are shorter than those in other previously described TiO phases and those of α -Ti^[28] (Table S6).

Among the TiO phases in the equilibrium Ti/O phase diagram,^[9] the β - and γ -phases are possible for a wide range of Ti/O molar ratios. On the other hand, the α -phase has a narrow composition range and is regarded as the stable phase at low temperatures. All of these TiO phases have both Ti and O structural defects. As the samples obtained here were mixtures of ϵ -TiO single crystals and γ/α -TiO grains, the density of ϵ -TiO could not be determined. The XRD-derived

molar volume of ϵ -TiO, however, is $12.47(2) \text{ cm}^3 \text{ mol}^{-1}$, postulating that there are no Ti or O defects. As shown in the electronic and thermodynamic stability studies below, the volume theoretically calculated for ϵ -TiO without Ti and O defects was $12.46 \text{ cm}^3 \text{ mol}^{-1}$ and hence identical to the experimental volume within one standard deviation. Clearly, the volume is much smaller than that of H-TiO ($15.46 \text{ cm}^3 \text{ mol}^{-1}$)^[21] and close to or slightly smaller than those of α -TiO ($12.92 \text{ cm}^3 \text{ mol}^{-1}$)^[20] and γ -TiO ($12.77 \text{ cm}^3 \text{ mol}^{-1}$).^[16] Table S6). As corroborated below, this suggests that ϵ -TiO, the highest-density TiO phase, is also the most stable one.

Full optimization of the ϵ -TiO structural model was carried out from first principles by using the Vienna ab initio simulation package (VASP)^[29,30] with the GGA-PBE functional^[31] and plane-wave basis sets generated by the PAW^[32,33] method (a detailed description and parameter listings for all theoretical parts of this study are given in the Supporting Information). The accuracy is excellent; for example, the theoretical Ti1–O and Ti2–O distances in ϵ -TiO arrive at 2.114 \AA and 1.978 \AA , which are to be compared with $2.1025(2) \text{ \AA}$ and $1.9745(8) \text{ \AA}$, respectively, as determined by XRD. Aside from the ground-state energies for α - and ϵ -TiO, the theoretical enthalpies of formation, $\Delta H_{f,\text{theo}}$, were also computed using the equation



and ab initio derived values for E_0 of crystalline Ti and “gaseous” O_2 ; the latter was modeled as a single molecule in a sufficiently large simulation cell to eliminate any interactions between periodic images. Strictly speaking, the enthalpy thus obtained is simplified as it is based on a model that uses gaseous O_2 at $T=0 \text{ K}$ without taking into account its sublimation enthalpy and heat capacity. Nonetheless, as our primary interest is a comparison of the TiO phases, this approach suffices to correctly evaluate enthalpic differences (and not absolute values). Furthermore, literature values were also obtained using the same method, allowing for a direct comparison.

All calculated values for $\Delta H_{f,\text{theo}}$ are given in Table S7. It is evident that irrespective of the individual calculation, the formation of ϵ -TiO ($\Delta H_{f,\text{theo}} = -513.7 \text{ kJ mol}^{-1}$) is energetically favored over α -TiO with an enthalpy difference of about 8 kJ mol^{-1} . Furthermore, the calculated $\Delta H_{f,\text{theo}}$ value for α -TiO ($-505.6 \text{ kJ mol}^{-1}$) is in very good agreement with the values reported by Graciani et al.^[12] and Andersson et al.^[13] but differs significantly from the one of Kostenko et al.,^[15] which was impossible to reproduce with either the VASP or the QuantumESPRESSO code.^[34] Nevertheless, the enthalpy difference is large enough to identify ϵ -TiO as the more stable ground-state phase. This finding is nicely reflected by a comparison of the total densities of states (DOS) of both polymorphs as determined by LOBSTER analysis^[35] (Figure 2). A local DOS minimum (a quasi band gap) at the Fermi level (E_F) was observed for ϵ -TiO, which was nearly half of the DOS of α -TiO at E_F and had a significantly different slope, indicating that the newly discovered phase is of larger electronic stability.

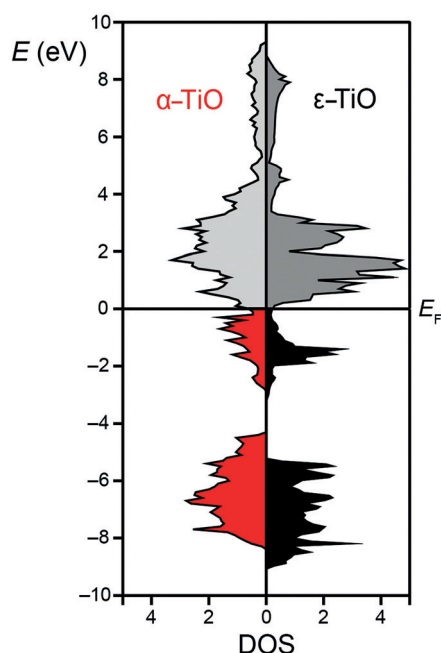


Figure 2. DOS plots for α - and ϵ -TiO. The gray regions correspond to unoccupied states located above the Fermi level.

To evaluate the thermodynamic stability of ϵ -TiO, it was analyzed by a quasiharmonic phonon calculation with PHONOPY^[36] using a $3 \times 3 \times 3$ supercell at equilibrium volume; the resulting phonon DOS is shown in Figure S6. Any structural instability would be revealed by imaginary modes but such frequencies were not found for ϵ -TiO. Hence, this structure is also mechanically stable. We restate that the theoretical molar volume of ϵ -TiO is $12.46 \text{ cm}^3 \text{ mol}^{-1}$ and thus clearly smaller than that of α -TiO ($13.12 \text{ cm}^3 \text{ mol}^{-1}$). This result is in line with the rule that more densely packed structures (ϵ -TiO) are energetically favored over less dense structures (α -TiO), as explained above.

The difference in the total energies of α - and ϵ -TiO is easily explained by an analysis of their chemical-bonding interactions. As described above, the α -phase is characterized by rather uncommon Ti/O polyhedra with fourfold (Ti1) and fivefold (Ti2 and Ti3) coordination and Ti–O distances of about 2.1 \AA , and there are also quite a few Ti–Ti contacts (ca. 2.9 \AA). In contrast, the ϵ -phase contains only two distinct Ti sites: Ti1 is coordinated by six O atoms (ca. 2.0 \AA) with a trigonal-prismatic arrangement whereas Ti2 has three nearest O neighbors (ca. 1.9 \AA) with a trigonal-planar arrangement; furthermore, there are fewer Ti–Ti contacts (for a list of these shortest interatomic contacts and their covalent bond strengths in terms of their integrated crystal orbital Hamilton populations (ICOHPs), which represent their contributions to the band-structure energy, see Table S8 and also below).

COHP^[37] analyses, performed with the TB-LMTO-ASA^[38,39] code and GGA-PW91 functional,^[40] for all Ti/O polyhedra of α -TiO (top) and ϵ -TiO (bottom) are shown in Figure 3a. Whereas there is indeed strong Ti–O bonding (green areas) in α -TiO for Ti1, Ti2, and also Ti3, somewhat

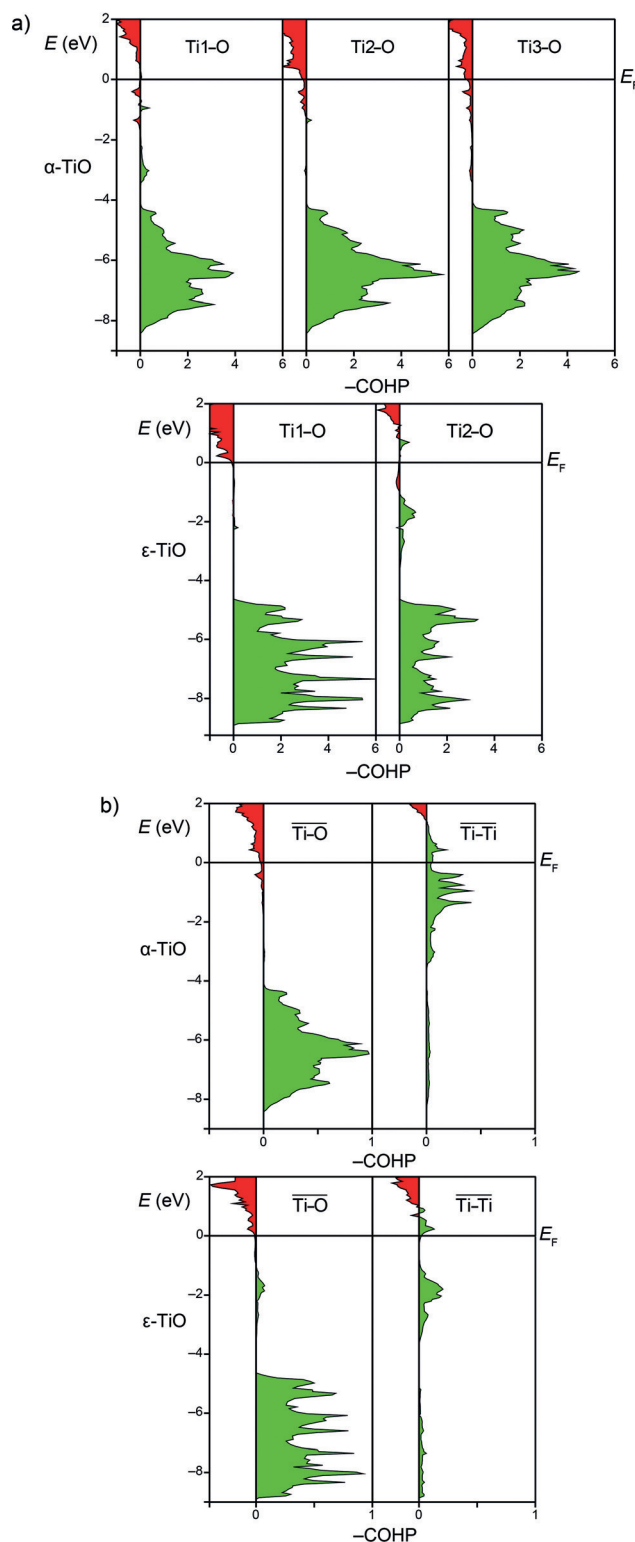


Figure 3. COHP diagrams. a) Ti–O bonds in the coordination polyhedra of α -TiO (top) and ϵ -TiO (bottom). Green and red areas signify bonding and antibonding interactions, respectively. The horizontal line labeled E_F shows the Fermi level. Scaling is identical in both diagrams. b) COHP bond strengths averaged over all Ti–O and Ti–Ti interactions in α - and ϵ -TiO irrespective of the crystallographic site. All interactions with $r < 3.0 \text{ \AA}$ were taken into account, and the sum was normalized to a single bond.

unexpectedly, there are also a few antibonding Ti–O interactions (small red areas) in the occupied region just below the Fermi level; the reason will be explained in a moment. For the more stable ϵ -TiO, the Ti–O interactions are (almost) exclusively bonding for Ti1 and Ti2. Therefore, the average Ti–O bond strength (in terms of the average ICOHP value) is larger in ϵ -TiO (–1.85 eV) than in α -TiO (–1.65 eV; see also Table S9).

The reason for the antibonding Ti/O states in α -TiO as opposed to ϵ -TiO can be visualized by plotting averaged COHPs, which now also include the Ti–Ti interactions (Figure 3b). The defective α -TiO structure (top) allows for a larger number of Ti–Ti contacts and bonding Ti–Ti interactions (in green) just below the Fermi level, and parts of the involved electrons are also contained in the (slightly) antibonding Ti/O states (on the left). On the other hand, ϵ -TiO is practically devoid of antibonding Ti–O interactions, and the amount of bonding Ti–Ti interactions is also smaller. Hence, the amount of heteropolar bonding (Ti–O) is larger in ϵ -TiO whereas homopolar bonding (Ti–Ti) is stronger in α -TiO; nonetheless, as heteropolar interactions are stronger than homopolar ones, metallic ϵ -TiO is the more stable, more ionic, more salt-like phase. All numerical information on the bonding strengths supports this claim (Table S10).

In conclusion, mixtures of single crystals of a new TiO polymorph (the so-called ϵ -phase) and grains of the known NaCl-type TiO phase have been synthesized by heating Ti metal in a Bi flux using Bi₂O₃ or TiO₂ as the oxygen source and by slowly cooling from 1173 K. The new polymorph can only be crystallized when a Bi flux is used. Single-crystal XRD data showed the new structure to be isotypic with ϵ -TaN (hexagonal *P6₂m*). First-principles electronic-structure calculations showed that the newly synthesized phase, ϵ -TiO, is more stable than α -TiO. Its energy, formation enthalpy, and the DOS at the Fermi level are lower, and its phonon DOS does not show any imaginary modes. The greater stability of ϵ -TiO is due to stronger heteropolar bonding than in α -TiO and the absence of antibonding Ti/O states below the Fermi level. The latter phase allows for stronger Ti–Ti bonding, which, however, cannot fully compensate the weaker Ti–O bonding. Therefore, metallic ϵ -TiO is the more stable, more ionic, and more salt-like polymorph of TiO.

Acknowledgements

We wish to thank Takashi Kamaya for WDX analysis and the IT Center of RWTH Aachen University for providing computational time and resources.

Keywords: chemical bonding · computational chemistry · phase stability · polymorphism · titanium monoxide

How to cite: *Angew. Chem. Int. Ed.* **2016**, *55*, 1652–1657
Angew. Chem. **2016**, *128*, 1684–1689

- [1] A. Fujishima, T. N. Rao, D. A. Tryk, *J. Photochem. Photobiol. C* **2000**, *1*, 1–21.

- [2] D. T. Cromer, K. Herrington, *J. Am. Chem. Soc.* **1955**, *77*, 4708–4709.
[3] B. Holmberg, *Acta Chem. Scand.* **1962**, *16*, 1245–1250.
[4] S. Andersson, B. Collén, U. Kuylenstierna, A. Magnéli, *Acta Chem. Scand.* **1957**, *11*, 1641–1652.
[5] S. Åsbrink, A. Magnéli, *Acta Crystallogr.* **1959**, *12*, 575–581.
[6] C. N. R. Rao, S. Ramdas, R. E. Loehman, J. M. Honig, *J. Solid State Chem.* **1971**, *3*, 83–88.
[7] C. E. Rice, W. R. Robinson, *Acta Crystallogr. Sect. B* **1977**, *33*, 1342–1348.
[8] Y. Le Page, P. Strobel, *J. Solid State Chem.* **1982**, *44*, 273–281.
[9] J. L. Murray, H. A. Wriedt, *Bull. Alloy Phase Diagrams* **1987**, *8*, 148–165.
[10] H. Okamoto, *J. Phase Equilib. Diffus.* **2011**, *32*, 473–474.
[11] H. Terauchi, J. B. Cohen, *J. Phys. Chem. Solids* **1978**, *39*, 681–686.
[12] J. Graciani, A. Márquez, J. F. Sanz, *Phys. Rev. B* **2005**, *72*, 054117.
[13] D. A. Andersson, P. A. Korzhavyi, B. Johansson, *Phys. Rev. B* **2005**, *71*, 144101.
[14] A. A. Valeeva, A. A. Rempel, W. Sprengel, H.-E. Schaefer, *Phys. Rev. B* **2007**, *75*, 094107.
[15] M. G. Kostenko, A. V. Lukoyanov, V. P. Zhukov, A. A. Rempel, *J. Solid State Chem.* **2013**, *204*, 146–152.
[16] M. D. Banus, T. B. Reed, A. J. Strauss, *Phys. Rev. B* **1972**, *5*, 2775–2784.
[17] E. Hilti, *Naturwissenschaften* **1968**, *55*, 130–131.
[18] E. Hilti, F. Laves, *Naturwissenschaften* **1968**, *55*, 131.
[19] D. Watanabé, J. R. Castles, A. Jostsons, A. S. Malin, *Acta Crystallogr.* **1967**, *23*, 307–313.
[20] H. Terauchi, J. B. Cohen, T. B. Read, *Acta Crystallogr. Sect. A* **1978**, *34*, 556–561.
[21] S. Möhr, H. Müller-Buschbaum, *Z. Anorg. Allg. Chem.* **1994**, *620*, 1175–1178.
[22] S. Andersson, *Acta Chem. Scand.* **1959**, *13*, 415–419.
[23] Bruker AXS, APEX2, v2014.11–10.
[24] G. M. Sheldrick, *Acta Crystallogr. Sect. A* **2008**, *64*, 112–122.
[25] K. Momma, F. Izumi, *J. Appl. Crystallogr.* **2008**, *41*, 653–658.
[26] A. N. Christensen, B. Lebech, *Acta Crystallogr. Sect. B* **1978**, *34*, 261–263.
[27] Crystal data for ϵ -TiO: crystal size: 0.110 × 0.029 × 0.027 mm³, space group *P6₂m* (No. 189), *a* = 4.9936(3) Å, *c* = 2.8773(2) Å, *V* = 62.136(9) Å³, *Z* = 3, ρ_{diff} = 5.123 g cm^{–3}, Bruker D8 Venture, Mo-K α radiation (0.71073 Å), numerical absorption correction, 9319 reflections, 359 independent reflections, *R*_{int} = 0.0410, least-squares refinement on *F*², *R* values (all data/*F*_o² ≥ 2σ(*F*_o²)): *R*₁ = 0.0125/0.0113, *wR*₂ = 0.0250/0.0241, GooF = 1.144, and 10 parameters. Further details on the crystal-structure investigations may be obtained from the Fachinformationszentrum Karlsruhe, 76344 Eggenstein-Leopoldshafen, Germany (fax: (+49) 7247-808-666; e-mail: crysdata@fiz-karlsruhe.de), on quoting the depository number CSD-430380.
[28] R. R. Pawar, V. T. Deshpande, *Acta Crystallogr. Sect. A* **1968**, *24*, 316–317.
[29] G. Kresse, J. Hafner, *Phys. Rev. B* **1993**, *47*, 558–561.
[30] G. Kresse, J. Furthmüller, *Comput. Mater. Sci.* **1996**, *6*, 15–50.
[31] J. P. Perdew, K. Burke, M. Ernzerhof, *Phys. Rev. Lett.* **1996**, *77*, 3865–3868.
[32] P. E. Blöchl, *Phys. Rev. B* **1994**, *50*, 17953–17979.
[33] G. Kresse, D. Joubert, *Phys. Rev. B* **1999**, *59*, 1758–1775.
[34] P. Giannozzi, S. Baroni, N. Bonini, M. Calandra, R. Car, C. Cavazzoni, D. Ceresoli, G. L. Chiarotti, M. Cococcioni, I. Dabo, A. D. Corso, S. Gironcoli, S. Fabris, G. Fratesi, R. Gebauer, U. Gerstmann, C. Gougousis, A. Kokalj, M. Lazzeri, L. Martin-Samos, N. Marzari, F. Mauri, R. Mazzarello, S. Paolini, A. Pasquarello, L. Paulatto, C. Sbraccia, S. Scandolo, G. Sclauzero, A. P. Seitsonen, A. Smogunov, P. Umari, R. M. J. Wentzcovitch, *Phys. Condens. Matter* **2009**, *21*, 395502.

- [35] S. Maintz, V. L. Deringer, A. L. Tchougréeff, R. Dronskowski, *J. Comput. Chem.* **2013**, *34*, 2557–2567.
- [36] A. Togo, I. Tanaka, *Scr. Mater.* **2015**, *108*, 1–5.
- [37] R. Dronskowski, P. E. Blöchl, *J. Phys. Chem.* **1993**, *97*, 8617–8624.
- [38] O. K. Andersen, *Phys. Rev. B* **1975**, *12*, 3060–3083.
- [39] O. K. Andersen, O. Jepsen, *Phys. Rev. Lett.* **1984**, *53*, 2571–2574.
- [40] J. P. Perdew, J. A. Chevary, S. H. Vosko, K. A. Jackson, M. R. Pederson, D. J. Singh, C. Fiolhais, *Phys. Rev. B* **1992**, *46*, 6671–6687.

Received: November 11, 2015

Published online: December 15, 2015